



HHS Public Access

Author manuscript

Exp Eye Res. Author manuscript; available in PMC 2019 January 01.

Published in final edited form as:

Exp Eye Res. 2018 January ; 166: 106–115. doi:10.1016/j.exer.2017.10.003.

Characterization of the Pleiotropic Roles of Sonic Hedgehog during Retinal Regeneration in Adult Zebrafish

Jennifer L. Thomas^a, Gregory W. Morgan^a, Kaylee M. Dolinski^a, and Ryan Thummel^{a,b}

^aDepartment of Anatomy and Cell Biology, Wayne State University School of Medicine, 540 E. Canfield, Detroit, MI, 48201, USA

^bDepartment of Ophthalmology, Wayne State University School of Medicine, 540 E. Canfield, Detroit, MI, 48201, USA

Abstract

In contrast to the mammalian retina, the zebrafish retina possesses the ability to regenerate. This is primarily accomplished through Müller glial cells, which, upon damage, re-enter the cell cycle to form retinal progenitors. The progenitors continue to proliferate as they migrate to the area of damage and ultimately differentiate into new neurons. The purpose of this study was to characterize the expression and function of Sonic Hedgehog (Shh) during regeneration of the adult zebrafish retina. Expression profiling of Shh pathway genes showed a significant upregulation of expression associated with stages of progenitor proliferation and neuronal differentiation. Activation of Shh signaling during early stages of retinal regeneration using intraocular injections of the recombinant human SHH (SHH-N) resulted in increased Müller cell gliosis, proliferation, and neuroprotection of damaged retinal neurons. Continued activation of Shh resulted in a greater number of differentiated amacrine and ganglion cells in the fully regenerated retina. Conversely, inhibition of Shh signaling using intraocular injections of cyclopamine resulted in decreased Müller glial cell proliferation and a fewer number of regenerated amacrine and ganglion cells. These data suggest that Shh signaling plays pleiotropic roles in proliferation and differentiation during adult zebrafish retinal regeneration.

Keywords

Sonic Hedgehog; Retina; Regeneration; Müller glia; Zebrafish; Cyclopamine

1. INTRODUCTION

Sonic Hedgehog (Shh) is one of three pattern-forming genes in the Hedgehog (Hh) signaling family. First discovered in *Drosophila* (Nusslein-Volhard and Wieschaus, 1980), Hh

Corresponding Author: Ryan Thummel, Ph.D., Department of Anatomy and Cell Biology, Department of Ophthalmology, Wayne State University School of Medicine, Detroit, USA, rthummel@med.wayne.edu, (313) 577-7762.

Publisher's Disclaimer: This is a PDF file of an unedited manuscript that has been accepted for publication. As a service to our customers we are providing this early version of the manuscript. The manuscript will undergo copyediting, typesetting, and review of the resulting proof before it is published in its final citable form. Please note that during the production process errors may be discovered which could affect the content, and all legal disclaimers that apply to the journal pertain.

All authors have no conflict of interest to declare.

necessary for rapid functional recovery following regeneration (Sherpa et al., 2014). The current study supports and extends these previous findings by defining the pleiotropic roles of Shh signaling during adult retinal regeneration in zebrafish. Specifically, we provide evidence that Shh signaling is required for a proper proliferation response from Müller glial cells following retinal damage. In addition, we show that Shh signaling also plays a role in progenitor differentiation by regulating the number of regenerated inner retinal neurons following damage. These data add to the growing body of literature that implicate Shh signaling as a critical factor during adult retinal regeneration in vertebrates.

2. MATERIALS AND METHODS

2.1 Zebrafish Lines and Maintenance

Wild-type *Danio rerio* (AB strain), Tg(*nrd:egfp*)/*alb* (Obholzer et al., 2008) and Tg(*gfap:egfp*)/*alb* (Kassen et al., 2007) were used for this study. Fish were fed a combination of brine shrimp and dried flake food three times daily and maintained at 28.5 °C on a 14 h light (250 lux): 10 h dark cycle (Westerfield, 1995). All animal care and experimental protocols used in this study were approved by the Institutional Animal Care and Use Committee at Wayne State University School of Medicine and are in compliance with the ARVO statement on the use of animals in vision research.

2.2 Light Lesion Protocol

Tg(*gfap:egfp*)/*alb* or Tg(*nrd:egfp*)/*alb* zebrafish (aged 6–12 months) were dark adapted for 10 days and exposed to an ultra-bright wide-spectrum light for 30-min (~100,000 lux) immediately followed by up to four days of exposure to constant bright light using the halogen lamps (250W; ~8000 lux) (Thomas et al., 2012a; Thomas and Thummel, 2013).

2.3 Intravitreal Injections

Intravitreal injections were performed as previously described (Qin et al., 2011; Thomas et al., 2016). Fish were anesthetized and a small incision was made in the cornea using a Safety Sideport Straight Knife (15°; Beaver-Vistec International). A 33-gauge blunt-end Hamilton Syringe was used to inject 0.5–0.75 microliters of solution. Ouabain injections (10 µM) were performed to damage all retinal neurons as previously described (Fimbel et al., 2007; Sherpa et al., 2014). Gain- and loss-of-function studies utilized 1X PBS or 1% EtOH for control solutions, and recombinant SHH-N protein (100 µg/mL in 1X PBS; R&D Systems) or cyclopamine (100 µM in 1% EtOH; Toronto Research Chemicals). Light damaged zebrafish were injected beginning at 2 days prior to light onset (– 2dpL) and continued daily through 2 dpL, with a maximum of 5 total injections (Suppl. Fig. 1A). Ouabain damaged retinas were injected beginning at 3 dpi and continued through 10 dpi, with a maximum of 8 total injections (Suppl Fig 1B).

2.4 Immunohistochemistry and Confocal Microscopy

Embryos and adult tissue was harvested and fixed in either 9:1 ethanolic formaldehyde (100% ethanol: 36% formaldehyde) overnight at 4° C. Tissues were then cryoprotected in 5% sucrose/1XPBS twice at room temperature, followed by a 30% sucrose/1X PBS wash overnight at 4° C, frozen in Tissue Freezing Medium (TFM) (Triangle Biomedical Sciences,

Durham, NC) and cryosectioned at 14–16 microns. Sections were transferred to glass slides, dried for up to 2 hours at 56° C, and stored at –80 °C. Immunohistochemistry was performed as previously described (Thummel et al., 2008). Primary antibodies included: rabbit polyclonal anti-green fluorescent protein (GFP) antisera (1:1,500, Abcam, Cambridge, MA), mouse monoclonal anti-Proliferating Cell Nuclear Antigen (PCNA) antibody (1:1000, Sigma Chemical), mouse monoclonal glutamine synthetase (GS) antibody (1:500, Chemicon), mouse monoclonal HuC/D antibody (1:50, Invitrogen), rabbit polyclonal anti-PKC antisera (1:100, Santa Cruz), and mouse monoclonal Zpr-3 and Zpr-1 antibodies (1:200, Zebrafish International Resource Center, Eugene, OR). Secondary antibodies included AlexaFluor goat anti-primary 488 and 594 (1:500, Invitrogen, Grand Island, NY) and nuclei were labeled with TO-PRO-3 (TP3; 1:750, Invitrogen). Coverslips were mounted using ProLong Gold (Molecular Probes, Eugene, OR) and confocal microscopy was performed using a Leica TCS SP2 or SP8 confocal microscope. Images were obtained using the exact same settings between groups, equidistant from the margin and the optic nerve in both the dorsal and ventral halves of the retina. Confocal images from the central dorsal retina were obtained as described above using the exact same capture settings (a minimum of N=5 per treatment per time point). Quantification of immunolocalized cells (Fig. 3I, Fig. 5C, Fig. 5B, Fig. 7D) were obtained within a linear distance of 300 microns and plotted as average number of cells per retina. Statistical significances between two groups was determined using Student's *t*-test.

2.5 Quantification of Müller glial cell hypertrophy

For GFP intensity quantifications, the Tg(*gfap:egfp*) line was used to visualize EGFP-positive Müller glial cells within the retina. First, confocal images were obtained from retinal sections containing the optic nerve using the exact same capture settings for all retinas (N=5 per treatment group per time point). Next, ImageJ was used to analyze the GFP intensity per pixel within a 300 micron linear distance in the central dorsal retina spanning the thickness of the retina (Thomas et al., 2016). Raw data were plotted as average pixel intensity and statistical significances between two groups was determined using Student's *t*-test. For quantification of Müller glial cell soma hypertrophy in the absence of light damage, ImageJ was used to trace the area of GFP-positive Müller glial cell somas within the same 300 micron linear distance of the images described above. N=20 Müller glial cells were quantified per retinal section. The data were normalized to the values of the saline injected control retinas and plotted as average percent area of Müller glial cell soma. Statistical significances between two groups was determined using Student's *t*-test.

2.5 Cell Death Analysis

Terminal Transferase dUTP Nick End Labeling (TUNEL) assay was performed using the ApoAlert DNA fragmentation kit (Clontech, Mountain View, CA), with some minor modifications as previously described (Qin et al., 2011). Tissue from 1 or 3 dpL light damaged zebrafish retinas was permeabilized in ice-cold NaCitrate buffer (0.1% NaCitrate, 0.1% Triton X-100) in the freezer for 2 minutes. TdT reaction was performed at 37° C for 2 hours using biotinylated dNTPs (New England Biolabs, Ipswich, MA). Enzyme reaction was followed by AlexaFluor-conjugated StrepAvidin labeling (Molecular Probes). Confocal images from the central dorsal retina were obtained as described above using the exact same

capture settings (N=5 per treatment per time point). Quantification of TUNEL+ cells in the ONL were obtained within a linear distance of 300 microns and plotted as average number of cells per retina. Statistical significances between two groups was determined using Student's *t*-test.

2.7 Quantitative Real-Time PCR

All qPCR was performed in biological and technical triplicate. Total RNA was isolated from a pool of 4–7 retinas in 0.5 mL Trizol reagent (N=3 pools per timepoint). The primers used for qPCR were: *gpiA* (For: TCCAAGGAAACAAGCCAAGC; Rev: TTCCACATCACACCCTGCAC), *gli1* (For: AGCAGTGCGGATCTGATGC; Rev: TAGCTTCGGTCTCCACCTGG), *ptch2* (For: GTGCTTTTCATTGGACTGCT; Rev: GACTCCTCTCCTTGCTTCTC), *shha* (For: AGTCTTACCTTTTCGCATCCCC; Rev: GATGTCCTTGCCGTCTCCTC), *shhb* (For: ACGAAGGCAAATCACAAGG; Rev: CCAGTGGTTCATGACGGATA). SYBR green (Applied Biosystems) qPCR reaction was carried out in technical triplicate of each sample pool using a Mastercycler Ep Realplex (Eppendorf). A total reaction volume of 20 microliters was used, including 2 microliters of cDNA. Analysis was performed using the Livak $C(t)$ method (Livak and Schmittgen, 2001) and normalized to the expression of the housekeeping gene, *gpiA*. Statistical analysis was performed for the expression of each gene across the entire timecourse using a One-way ANOVA with post-hoc Tukey test. Statistical difference in expression relative to 0 hr expression levels were noted by an asterisk in the graphs ($p < 0.05$).

2.4 EdU Incorporation

59-ethynyl-29-deoxyuridine (EdU; Invitrogen, Carlsbad, CA) was diluted in 1XPBS to 1 mg/mL and injected intraperitoneally (IP; 50 microliters) into adult *Tg(nrd:egfp)/alb* zebrafish as previously described (Bailey et al., 2010). EdU injections began at 1 dpL and were repeated daily through 3 dpL. Immunolocalization of EdU was performed using Click-iT EdU AlexaFluor 594 Imaging Kit per the manufacturer's instructions (Invitrogen), followed by GFP immunolocalization. Confocal images from the central dorsal retina were obtained as described above using the exact same capture settings (N=5 per treatment per time point). Quantification of EdU+ cells in the INL and ONL at 11 dpL were obtained within a linear distance of 300 microns and plotted as average number of cells per retina. Statistical significances between two groups was determined using Student's *t*-test.

3. RESULTS

3.1 Expression of *shh* signaling pathway genes during retinal regeneration

We performed quantitative real-time PCR (qPCR) to determine the expression profiles of *shha*, *shhb*, *gli1* and *ptch2* following phototoxic damage to adult zebrafish retinas. In addition, immunolocalization of the proliferation marker PCNA was performed at 1.5, 3, and 7 days post-light onset (dpL; Fig. 1A–D) to confirm that these collection times corresponded to Müller glial cell cycle reentry (1.5 dpL), progenitor amplification and migration (3 dpL), and a quiescence of the proliferation response (7 dpL). Undamaged (0 dpL) retinas were used as a negative control. Expression analysis of *shha* and *shhb* by qPCR showed no change in expression at 1.5 dpL, but a significant upregulation of expression at 3 and 7 dpL (Fig.

1E). Expression of *gli1* increased in expression from 0 to 3 dpL, but did not reach statistical significance (Fig. 1E). However, like *shha* and *shhb*, expression of *ptch2* was significantly upregulated at 3 dpL (Fig. 1E).

Next, we used a high dose of the neurotoxin Ouabain to characterize *shh* expression following the complete loss of retinal neurons (Fimbel et al., 2007; Maier and Wolburg, 1979; Sherpa et al., 2014). In addition, immunohistochemical markers were used to confirm that Ouabain destroyed retinal neurons in a progressive manner, moving from the inner to the outer retina, and that the Müller glial cells remained to re-enter the cell cycle. Specifically, at 1 day following Ouabain injection (dpi), HuC/D-positive ganglion cells were lost (Fig. 2B) and a massive expansion of the inner plexiform layer (IPL) was visualized by Glutamine Synthetase immunolocalization to Müller glial cells (Fig. 2N). At 3 dpi, the majority of amacrine cells were lost (Fig. 2C) and Müller glial cells reentered the cell cycle (Fig. 2U). At 7 dpi, photoreceptor loss was observed (Fig. 2J) and Müller glial cells collapsed and surrounded large numbers of proliferating retinal progenitors (Fig. 2P, V). Partial regeneration of both inner and outer retinal neurons was visualized by 14 dpi, and the retina appeared fully regenerated by 60 dpi (Figure 2E, F, K, L). Expression analysis of *shha* and *shhb* by qPCR showed a significant upregulation of both genes at 3 and 14 dpi (Fig. 2Y), corresponding to time points when Müller glial cells reentered the cell cycle and when differentiation of new neurons was observed, respectively. This is in contrast to a previous report that *shha* expression is down-regulated at 3 and 12 dpi of Ouabain (Sherpa et al., 2014). Expression of *gli1*, in contrast, remained significantly elevated from 1–28 dpi, whereas expression of *ptch2* levels did not reach significance at any time point (Fig. 2Y).

3.2 Shh Signaling Regulates Müller Glial Cell Proliferation

In order to explore the role of Shh signaling during retinal regeneration, gain-and-loss of function experiments were performed using intravitreal injections of recombinant SHH (SHH-N) and cyclopamine. These experiments were performed in the Tg(*gfap:egfp*) line, which allows for clear visualization of the cellular morphology Müller glia. In the absence of damage, no apparent changes to Müller cell morphology were observed following intravitreal injections of saline or cyclopamine (Fig. 3A, C). However, retinas injected with SHH-N exhibited Müller glial cells with cellular hypertrophy (Fig. 3B) (Thomas et al., 2016), characterized by a significant increase in GFP intensity and Müller glial cell soma area when compared with saline injected control retinas (Fig. 3A–B; G–H). This phenotype persisted through 1.5 dpL, when Müller glial cells re-entered the cell cycle (Fig. 3D–F, G). In addition, compared with saline-injected retinas at 1.5 dpL, SHH-N treated retinas contained a significantly greater percentage of Müller glial cells that reentered the cell cycle (Fig. 3E, I). Conversely, cyclopamine treated retinas contained a significantly reduced percentage of Müller glial cells that reentered the cell cycle at 1.5 dpL (Fig. 3F, I). These data show that manipulating Shh signaling during retinal regeneration results in changes to Müller glial cell proliferation.

3.3 Shh is Neuroprotective to Photoreceptors

In the previous experiment, we noted that retinas injected with SHH-N exhibited hypertrophied Müller glial cell appendages within a relatively thicker outer nuclear layer

(ONL) than saline-injected control retinas at 1.5 dpL (compare Fig. 3D with 3E). To explore the possibility that SHH-N injections resulted in neuroprotection from the phototoxic damage, we first analyzed light damaged retinas for apoptosis at 1 and 3 dpL by TUNEL analysis. At 1 dpL, the peak stage of photoreceptor apoptosis, significantly fewer TUNEL-positive nuclei were observed in the ONL of SHH-N-treated retinas (Fig. 4AB, E). At 3 dpL, when photoreceptor loss was largely complete in control retinas, no differences were observed between the groups (Fig. 4C–E). This suggests that SHH-N treatment did not simply delay cell death. Next, we immunolabeled light-damaged retinas for markers of rod and cone photoreceptors. At 3 dpL, nearly all rod and cone photoreceptors were destroyed by the photolytic damage in control retinas, which was followed by an increased number of newly-regenerated photoreceptors at 7 and 11 dpL (Fig. 5A–C). In contrast, SHH-N-treated retinas maintained high numbers of rod and cone photoreceptors throughout the light treatment timecourse (Fig. 5A–C), consistent with it playing a neuroprotective role. It is currently unclear, however, whether this neuroprotection is mediated through Müller glial cell activation (i.e. indirect action) or by directly effecting retinal neurons.

3.4 Shh Signaling Regulates the Regeneration of Inner Retinal Neurons

In order to test whether SHH-N treatment had any effect on later stages of progenitor differentiation, we first quantified retinal thickness and retinal nuclei at 11 dpL. SHH-N-treated retinas possessed a thicker INL that contained significantly more inner retinal neurons than saline-injected control retinas (Fig. 6A–B). In contrast, no significant change in cell number was observed following treatment with cyclopamine (data not shown; EtOH control=472.20±60.52, Cyc=405.00±22.34; $p=0.291$). Next, EdU labeling was performed to label the proliferating retinal progenitors at 3 dpL and their progeny at 11 dpL (Bailey et al., 2010; Thomas et al., 2012b). In control retinas, EdU labeling was visualized in columns of progenitor cells as they migrated from the INL to the ONL at 3 dpL, and in regenerated rods and cones in the ONL at 11 dpL (Fig. 6C, D). In contrast, EdU-positive cells in SHH-N-treated retinas remained largely in the INL at both time points, with significantly fewer EdU-labeled cells in the ONL at 11 dpL (Fig. 6C, D). Although a few PKC-positive/EdU-positive bipolar cells were observed (Fig. 6E), HuC/D immunolabeling showed that the majority of EdU-positive cells that remained in the INL at 11 dpL were amacrine cells (Fig. 6E).

Together, these data show that SHH-N treated retinas generated an excess of unneeded retinal progenitors that largely remained in the INL and differentiated into an excess of inner retinal neurons, raising the possibility that excess Shh activity drove the unneeded progenitors to an amacrine or ganglion cell fate. However, an alternative explanation is that EdU-positive INL progenitors did not migrate to the ONL because regeneration of the photoreceptors was not necessary or because excess Shh signaling prevented the migration of progenitors from the INL to the ONL. In order to test these possibilities and determine whether differentiation of other cell types was affected by SHH-N, we used the Ouabain damage model to damage all retinal neurons (Fimbel et al., 2007; Sherpa et al., 2014). At 7 dpi, both inner and outer retinal neurons of saline, SHH-N, and cyclopamine-injected retinas were lost (Fig. 7A, D). At 11 dpi, SHH-N-treated retinas possessed significantly more amacrine and ganglion cells, while cyclopamine-treated retinas possessed significantly fewer (Fig. 7A, D). Cyclopamine-treated retinas possessed a very thin inner plexiform layer,

whereas SHH-N-treated retinas possessed an expanded and disorganized inner plexiform layer that contained misplaced inner retinal neurons (Fig. 7A). No significant change in the number of regenerated photoreceptors in the ONL was observed between the control and treatment groups (Fig. 7B–D). However, SHH-N-treated retinas possessed rosettes of immunolabeled photoreceptors in the INL (Fig. 7B–C). In general, these phenotypes did not recover at 28 dpi; the number of amacrine and ganglion cells remained significantly increased in SHH-N-treated retinas and significantly decreased in cyclopamine-treated retinas (Fig. 7A, D). Together, these data suggest that Shh signaling is both sufficient and necessary to drive retinal progenitors toward an inner retinal neuron cell fate.

4. DISCUSSION

Different factors have been suggested as regulators of cell proliferation in the retina, including *Ascla*, *H-EGF*, *Wnt*, and *Shh* (Liu et al., 2013; Ramachandran et al., 2011; Sun et al., 2014; Wan et al., 2012). The Sonic Hedgehog (Shh) signaling pathway is conserved from invertebrates, is essential for proper retinal development in all vertebrates, and has been implicated as a key regulator of proliferation following photoreceptor damage in the mammalian retina (Wan et al., 2007). Furthermore, in the damaged chick retina, pharmacological activation of Shh stimulated proliferation of Müller glial-derived progenitor cells. Finally, in the damaged adult zebrafish retina, cyclopamine inhibition of the Shh signaling pathway reduced the rate of progenitor cell proliferation, while indirect activation of the Shh pathway by knockdown of *Stil* increased the rate of cell proliferation (Sun et al., 2014), demonstrating a role for the endogenous Shh pathway during retinal regeneration. Our findings confirm that Shh signaling is required for a proper proliferation response from Müller glial cells following retinal damage and that overexpression of the Shh pathway by SHH-N injections results in excess proliferation. In addition, we showed that SHH-N treatment resulted in extremely reactive Müller glia based on hypertrophied somas and appendages, and an upregulation of the *gfap:egfp* transgene (Fig. 3). We have previously demonstrated that Müller glia in the adult zebrafish initiate a gliotic response immediately following damage to adult retinal neurons, but that this response is transient and is restricted to the area of damage (e.g. the ONL during phototoxic damage) (Thomas et al., 2016). Interestingly, SHH-N induced Müller glial reactivity throughout all retinal layers and induced reactivity even in the absence of damage (Fig. 3B). Furthermore, during phototoxic damage to the retinal photoreceptors, SHH-N treated Müller glia remained highly reactive as they re-entered the cell cycle (Fig. 3E). These data demonstrate that zebrafish Müller glia have the ability to be simultaneously proliferating and persistently reactive and that SHH-N induced a characteristic reactive gliosis response coupled with uncontrolled proliferation. Given that this gliotic/proliferation response is similar to that observed in proliferative retinopathies of the mammalian retina following severe retinal damage, future studies will explore the extent to which SHH-N treatment represents a valid model for exploring these phenotypes.

In addition to a role in gliosis and proliferation, we provide evidence that Shh signaling plays a role in progenitor cell differentiation during retinal regeneration. First, we showed that SHH-N treatment during light treatment resulted in progenitors that largely failed to migrate to the ONL and instead differentiated into an excess of inner retinal neurons (Figs. 5

and 6). These findings suggest that SHH-N treatment either prevented progenitor cell migration or directed progenitor cells towards an inner retinal cell fate. We therefore repeated this experiment in the Ouabain damage model, where all retinal neurons are damaged and progenitors migrate to repopulate both the inner and outer retinal layers (Fimbel et al., 2007; Sherpa et al., 2014; Thomas et al., 2016). Again, we found that SHH-N treatment resulted in an excess of inner retinal neurons and that cyclopamine resulted in reduced numbers of inner retinal neurons. These findings suggest that excess Shh signaling did not affect progenitor cell migration, but rather, drove progenitors toward an inner retinal neuron cell fate. These results are consistent with the known role of Shh signaling during vertebrate retinal development, during which Shh secretion induces the wave of amacrine and ganglion cell differentiation (Neumann and Nuesslein-Volhard, 2000; Sanchez-Arrones et al., 2013; Sanchez-Camacho and Bovolenta, 2008; Shkumatava et al., 2004; Shkumatava and Neumann, 2005). Importantly, in both treatment groups, we observed that progenitors properly repopulated the photoreceptors in normal numbers (Fig. 7D). However, overexpression of Shh resulted in the formation of rosettes in the INL that specifically express rod and cone opsins, whereas inhibiting Shh signaling eliminates this phenotype (Fig. 7C). These results are consistent with findings in the damaged mammalian retina, whereby unregulated proliferation can lead to an excess of de-differentiated and misplaced neurons in the inner retina (Lewis et al., 2010). However, the exact mechanism that underlies this phenotype remains a matter of speculation.

Some differences between the light and Ouabain damage models were noted, even in the absence of altered Shh activity. It is well established that in the light damage model, significant loss to the outer retina occurs by 1 dpL, and conversely, in the Ouabain damage model, significant loss to the inner retina occurs by 1 dpi (Kassen et al., 2007; Sherpa et al., 2008; Sherpa et al., 2014; Thomas et al., 2012a; Thummel et al., 2008). However, in the light damage model Müller glial cells re-enter the cell cycle at 1.5 dpL, whereas in the Ouabain damage model, Müller glial cells do not re-enter the cell cycle until 3 dpi (Figs. 1–2), suggesting that there are different “activating” molecules that are released from dying inner and outer retinal neurons. With regard to Shh expression, we observed that *shha* and *shhb* were upregulated in both models concomitant with Müller glial cell re-entry, but not prior (Figs. 1–2). Expression of *gli1* was upregulated prior to Müller glial cell re-entry in the Ouabain damage model, but not in the light damage model (Figs. 1–2). Finally, *ptch2* expression was upregulated in the light damage model at 3 dpL, but did not reach significance in the Ouabain damage model at any time point tested (Fig. 1–2). Therefore, similarities and differences in Shh activity appear to be present in each damage model.

We also noted differences from a previously published report (Sherpa et al., 2014) in regard to *shha* expression following Ouabain damage. Sherpa and colleagues compared the effects of two doses of Ouabain (2 and 10 μ M) on retinal damage and regeneration in zebrafish, in which the lower dose resulted in selective damage to inner retinal neurons, and the higher dose resulted in significant damage to all layers of the retina. They found a near-identical decrease in *shha* expression at 3 and 5 dpi with both doses. In contrast, our analysis using the higher dose showed a significant increase in *shha* expression at 3 dpi and no change at 5 dpi (Fig. 2). The majority of cell loss occurs between 3 and 7 dpi using 10 μ M Ouabain, with the damage spreading from the inner to the outer retina (Fig. 2). One potential explanation

for our finding that *shha* increased at 3 dpi is that a greater number of *shha*-expressing cells “escaped” Ouabain damage in our hands than in the previous report at 3 dpi. This is consistent with the fact that Sherpa and colleagues showed significant decreases in expression of all markers of ganglion cells at 3 dpi, suggestive that these cells were completely destroyed in their hands. Therefore, a selectively greater number of living cells that express *shha* at 3 dpi in our findings could account for the increase that we observed compared with the previous report and may represent a last attempt of the damaged inner retinal neurons to increase Shh signaling prior to death.

In conclusion, this study characterizes the pleiotropic roles for Shh signaling following constant-intense light and Ouabain damage. We show that Shh signaling is required for Müller glial cell proliferation early, followed by properly regulating inner retinal neuron differentiation. These data add Shh to the growing list of cell signaling pathways that regulate Müller glial dedifferentiation and proliferation (Lenkowski et al., 2013; Nelson et al., 2013; Ramachandran et al., 2011; Thummel et al., 2010; Wan et al., 2012). While it is clear that Shh signaling regulates Müller glial cell proliferation, more extensive studies are needed to determine where Shh signaling integrates into existing pathways of regulation and which of the herein-described phenotypes are a result of direct or indirect regulation by Shh. Furthermore, these data suggest that caution should be given to only searching for molecules that effect Müller glial proliferation without looking at the effect on long-term regeneration. If, like Shh, a given molecule plays pleiotropic roles during retinal regeneration, then its continued overexpression would likely have negative outcomes on the overall regeneration response.

Supplementary Material

Refer to Web version on PubMed Central for supplementary material.

Acknowledgments

The authors would like to thank Xixia Luo for excellent fish husbandry and technical support. This work was funded by the National Institutes of Health grants R01EY026551, P30EY04068 and start-up funds to RT, including an unrestricted grant from Research to Prevent Blindness to the Wayne State University, Department of Ophthalmology. JT was supported by a Thomas C. Rumble Fellowship provided by the Wayne State University Graduate School.

References

- Bailey TJ, Fossum SL, Fimbel SM, Montgomery JE, Hyde DR. The inhibitor of phagocytosis, O-phospho-L-serine, suppresses Muller glia proliferation and cone cell regeneration in the light-damaged zebrafish retina. *Experimental eye research*. 2010; 91:601–612. [PubMed: 20696157]
- Bellusci S, Furuta Y, Rush MG, Henderson R, Winnier G, Hogan BL. Involvement of Sonic hedgehog (Shh) in mouse embryonic lung growth and morphogenesis. *Development*. 1997; 124:53–63. [PubMed: 9006067]
- Chiang C, Litingtung Y, Lee E, Young KE, Corden JL, Westphal H, Beachy PA. Cyclopia and defective axial patterning in mice lacking Sonic hedgehog gene function. *Nature*. 1996; 383:407–413. [PubMed: 8837770]
- Ericson J, Muhr J, Jessell TM, Edlund T. Sonic hedgehog: a common signal for ventral patterning along the rostrocaudal axis of the neural tube. *The International journal of developmental biology*. 1995; 39:809–816. [PubMed: 8645565]

- Fimbel SM, Montgomery JE, Burket CT, Hyde DR. Regeneration of inner retinal neurons after intravitreal injection of ouabain in zebrafish. *J Neurosci.* 2007; 27:1712–1724. [PubMed: 17301179]
- Hu M, Easter SS. Retinal neurogenesis: the formation of the initial central patch of postmitotic cells. *Developmental biology.* 1999; 207:309–321. [PubMed: 10068465]
- Johnson RL, Tabin C. The long and short of hedgehog signaling. *Cell.* 1995; 81:313–316. [PubMed: 7736584]
- Kassen SC, Ramanan V, Montgomery JE, C TB, Liu CG, Vihtelic TS, Hyde DR. Time course analysis of gene expression during light-induced photoreceptor cell death and regeneration in albino zebrafish. *Developmental neurobiology.* 2007; 67:1009–1031. [PubMed: 17565703]
- Katoh Y, Katoh M. Integrative genomic analyses on GLI1: positive regulation of GLI1 by Hedgehog-GLI, TGFbeta-Smads, and RTK-PI3K-AKT signals, and negative regulation of GLI1 by Notch-CSL-HES/HEY, and GPCR-Gs-PKA signals. *International journal of oncology.* 2009; 35:187–192. [PubMed: 19513567]
- Krauss S, Concordet JP, Ingham PW. A functionally conserved homolog of the *Drosophila* segment polarity gene *hh* is expressed in tissues with polarizing activity in zebrafish embryos. *Cell.* 1993; 75:1431–1444. [PubMed: 8269519]
- Laufer E, Nelson CE, Johnson RL, Morgan BA, Tabin C. Sonic hedgehog and Fgf-4 act through a signaling cascade and feedback loop to integrate growth and patterning of the developing limb bud. *Cell.* 1994; 79:993–1003. [PubMed: 8001146]
- Lenkowski JR, Qin Z, Sifuentes CJ, Thummel R, Soto CM, Moens CB, Raymond PA. Retinal regeneration in adult zebrafish requires regulation of TGFbeta signaling. *Glia.* 2013; 61:1687–1697. [PubMed: 23918319]
- Lewis GP, Chapin EA, Luna G, Linberg KA, Fisher SK. The fate of Muller's glia following experimental retinal detachment: nuclear migration, cell division, and subretinal glial scar formation. *Molecular Vision.* 2010; 16:1361–1372. [PubMed: 20664798]
- Liu B, Hunter DJ, Rooker S, Chan A, Paulus YM, Leucht P, Nusse Y, Nomoto H, Helms JA. Wnt signaling promotes Muller cell proliferation and survival after injury. *Investigative ophthalmology & visual science.* 2013; 54:444–453. [PubMed: 23154457]
- Livak KJ, Schmittgen TD. Analysis of relative gene expression data using real-time quantitative PCR and the 2(-Delta Delta C(T)) Method. *Methods.* 2001; 25:402–408. [PubMed: 11846609]
- Maier W, Wolburg H. Regeneration of the goldfish retina after exposure to different doses of ouabain. *Cell and tissue research.* 1979; 202:99–118. [PubMed: 509506]
- Masai I, Stemple DL, Okamoto H, Wilson SW. Midline signals regulate retinal neurogenesis in zebrafish. *Neuron.* 2000; 27:251–263. [PubMed: 10985346]
- McMahon AP. More surprises in the Hedgehog signaling pathway. *Cell.* 2000; 100:185–188. [PubMed: 10660040]
- Murone M, Rosenthal A, de Sauvage FJ. Sonic hedgehog signaling by the patched-smoothed receptor complex. *Current biology: CB.* 1999; 9:76–84. [PubMed: 10021362]
- Nelson CM, Ackerman KM, O'Hayer P, Bailey TJ, Gorsuch RA, Hyde DR. Tumor necrosis factor-alpha is produced by dying retinal neurons and is required for Muller glia proliferation during zebrafish retinal regeneration. *J Neurosci.* 2013; 33:6524–6539. [PubMed: 23575850]
- Neumann CJ, Nusslein-Volhard C. Patterning of the zebrafish retina by a wave of sonic hedgehog activity. *Science.* 2000; 289:2137–2139. [PubMed: 11000118]
- Nusslein-Volhard C, Wieschaus E. Mutations affecting segment number and polarity in *Drosophila*. *Nature.* 1980; 287:795–801. [PubMed: 6776413]
- Obholzer N, Wolfson S, Trapani JG, Mo W, Nechiporuk A, Busch-Nentwich E, Seiler C, Sidi S, Sollner C, Duncan RN, Boehland A, Nicolson T. Vesicular glutamate transporter 3 is required for synaptic transmission in zebrafish hair cells. *J Neurosci.* 2008; 28:2110–2118. [PubMed: 18305245]
- Pillai-Kastoori L, Wen W, Wilson SG, Strachan E, Lo-Castro A, Fichera M, Musumeci SA, Lehmann OJ, Morris AC. Sox11 is required to maintain proper levels of Hedgehog signaling during vertebrate ocular morphogenesis. *PLoS genetics.* 2014; 10:e1004491. [PubMed: 25010521]

- Qin Z, Kidd AR 3rd, Thomas JL, Poss KD, Hyde DR, Raymond PA, Thummel R. FGF signaling regulates rod photoreceptor cell maintenance and regeneration in zebrafish. *Experimental eye research*. 2011; 93:726–734. [PubMed: 21945172]
- Ramachandran R, Zhao XF, Goldman D. *Ascl1a/Dkk/beta-catenin signaling pathway is necessary and glycogen synthase kinase-3beta inhibition is sufficient for zebrafish retina regeneration*. *Proceedings of the National Academy of Sciences of the United States of America*. 2011; 108:15858–15863. [PubMed: 21911394]
- Roberts DJ, Johnson RL, Burke AC, Nelson CE, Morgan BA, Tabin C. Sonic hedgehog is an endodermal signal inducing *Bmp-4* and *Hox* genes during induction and regionalization of the chick hindgut. *Development*. 1995; 121:3163–3174. [PubMed: 7588051]
- Sanchez-Arrones L, Nieto-Lopez F, Sanchez-Camacho C, Carreres MI, Herrera E, Okada A, Bovolenta P. *Shh/Boc signaling is required for sustained generation of ipsilateral projecting ganglion cells in the mouse retina*. *J Neurosci*. 2013; 33:8596–8607. [PubMed: 23678105]
- Sanchez-Camacho C, Bovolenta P. *Autonomous and non-autonomous Shh signalling mediate the in vivo growth and guidance of mouse retinal ganglion cell axons*. *Development*. 2008; 135:3531–3541. [PubMed: 18832395]
- Sherpa T, Fimbel SM, Mallory DE, Maaswinkel H, Spritzer SD, Sand JA, Li L, Hyde DR, Stenkamp DL. *Ganglion cell regeneration following whole-retina destruction in zebrafish*. *Developmental neurobiology*. 2008; 68:166–181. [PubMed: 18000816]
- Sherpa T, Lankford T, McGinn TE, Hunter SS, Frey RA, Sun C, Ryan M, Robison BD, Stenkamp DL. *Retinal regeneration is facilitated by the presence of surviving neurons*. *Developmental neurobiology*. 2014; 74:851–876. [PubMed: 24488694]
- Shkumatava A, Fischer S, Muller F, Strahle U, Neumann CJ. *Sonic hedgehog, secreted by amacrine cells, acts as a short-range signal to direct differentiation and lamination in the zebrafish retina*. *Development*. 2004; 131:3849–3858. [PubMed: 15253932]
- Shkumatava A, Neumann CJ. *Shh directs cell-cycle exit by activating p57Kip2 in the zebrafish retina*. *EMBO Rep*. 2005; 6:563–569. [PubMed: 15891769]
- Stenkamp DL, Frey RA, Prabhudesai SN, Raymond PA. *Function for Hedgehog genes in zebrafish retinal development*. *Developmental biology*. 2000; 220:238–252. [PubMed: 10753513]
- Sun L, Li P, Carr AL, Gorsuch R, Yarka C, Li J, Bartlett M, Pfister D, Hyde DR, Li L. *Transcription of the SCL/TAL1 interrupting Locus (Stil) is required for cell proliferation in adult Zebrafish Retinas*. *The Journal of biological chemistry*. 2014; 289:6934–6940. [PubMed: 24469449]
- Thomas JL, Nelson CM, Luo X, Hyde DR, Thummel R. *Characterization of multiple light damage paradigms reveals regional differences in photoreceptor loss*. *Experimental eye research*. 2012a; 97:105–116. [PubMed: 22425727]
- Thomas JL, Ochocinska MJ, Hitchcock PF, Thummel R. *Using the Tg(nrd:egfp)/albino zebrafish line to characterize in vivo expression of neurod*. *PLoS one*. 2012b; 7:e29128. [PubMed: 22235264]
- Thomas JL, Ranski AH, Morgan GW, Thummel R. *Reactive gliosis in the adult zebrafish retina*. *Experimental eye research*. 2016; 143:98–109. [PubMed: 26492821]
- Thomas JL, Thummel R. *A novel light damage paradigm for use in retinal regeneration studies in adult zebrafish*. *Journal of visualized experiments: JoVE*. 2013:e51017. [PubMed: 24192580]
- Thummel R, Enright JM, Kassen SC, Montgomery JE, Bailey TJ, Hyde DR. *Pax6a and Pax6b are required at different points in neuronal progenitor cell proliferation during zebrafish photoreceptor regeneration*. *Experimental eye research*. 2010; 90:572–582. [PubMed: 20152834]
- Thummel R, Kassen SC, Enright JM, Nelson CM, Montgomery JE, Hyde DR. *Characterization of Muller glia and neuronal progenitors during adult zebrafish retinal regeneration*. *Experimental eye research*. 2008; 87:433–444. [PubMed: 18718467]
- Todd L, Fischer AJ. *Hedgehog signaling stimulates the formation of proliferating Muller glia-derived progenitor cells in the chick retina*. *Development*. 2015; 142:2610–2622. [PubMed: 26116667]
- Todd L, Volkov LI, Zelinka C, Squires N, Fischer AJ. *Heparin-binding EGF-like growth factor (HB-EGF) stimulates the proliferation of Muller glia-derived progenitor cells in avian and murine retinas*. *Molecular and cellular neurosciences*. 2015; 69:54–64. [PubMed: 26500021]
- Tsukiji N, Amano T, Shiroishi T. *A novel regulatory element for Shh expression in the lung and gut of mouse embryos*. *Mechanisms of development*. 2014; 131:127–136. [PubMed: 24157522]

- Wan J, Ramachandran R, Goldman D. HB-EGF is necessary and sufficient for Muller glia dedifferentiation and retina regeneration. *Developmental cell*. 2012; 22:334–347. [PubMed: 22340497]
- Wan J, Zheng H, Xiao HL, She ZJ, Zhou GM. Sonic hedgehog promotes stem-cell potential of Muller glia in the mammalian retina. *Biochem Biophys Res Commun*. 2007; 363:347–354. [PubMed: 17880919]
- Wang Y, Dakubo GD, Thurig S, Mazerolle CJ, Wallace VA. Retinal ganglion cell-derived sonic hedgehog locally controls proliferation and the timing of RGC development in the embryonic mouse retina. *Development*. 2005; 132:5103–5113. [PubMed: 16236765]
- Westerfield. *The Zebrafish Book: A guide for the laboratory use of zebrafish (Danio rerio)*. Univ of Oregon Press; Eugene, OR: 1995.
- Zhang XM, Yang XJ. Regulation of retinal ganglion cell production by Sonic hedgehog. *Development*. 2001; 128:943–957. [PubMed: 11222148]

Highlights

- Shh signaling induces Müller cell gliosis
- Shh regulates the percentage of Müller glial cells that re-enter the cell cycle following damage
- Shh signaling regulates the regeneration of inner retinal neurons

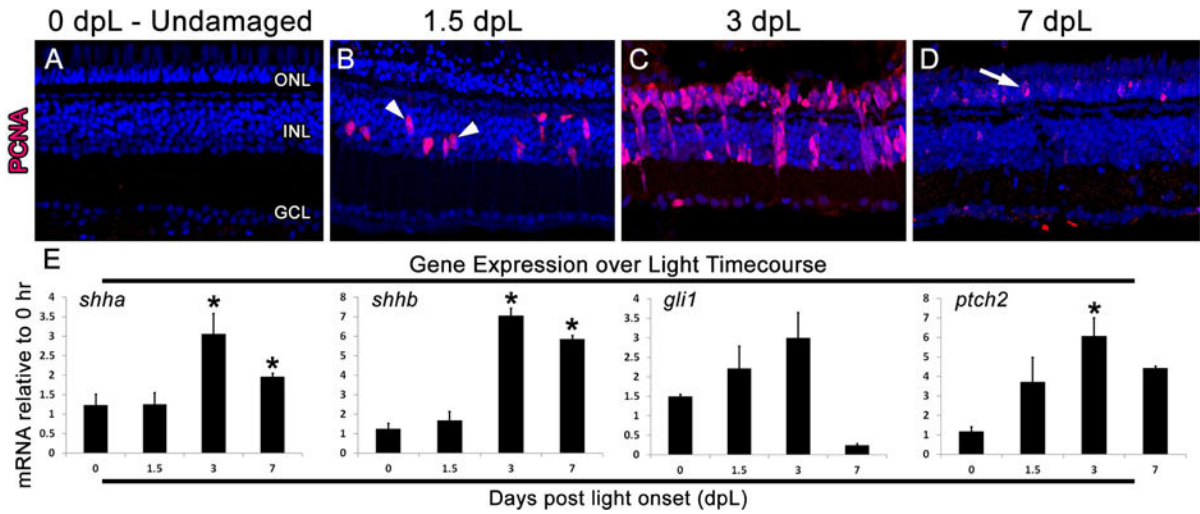
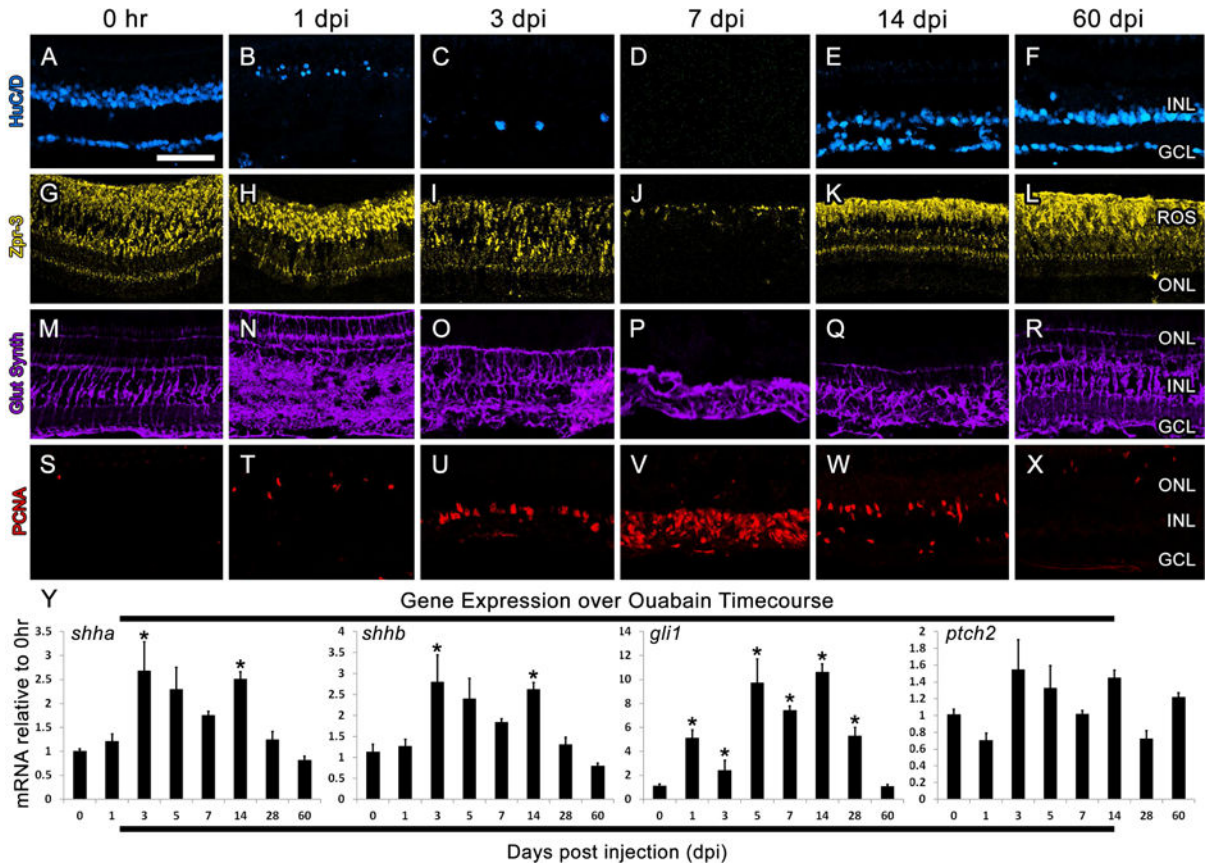


Figure 1. Expression of *shh* signaling pathway genes in the light damaged zebrafish retina
 A–D) Retinal sections from light damaged zebrafish at 0, 1.5, 3, and 7 days post light onset (dpL) immunolabeled with PCNA (red) to show cell proliferation and a nuclear stain (blue). A subset of Müller glia re-entered the cell cycle at 1.5 dpL (arrowheads; panel B) and produce large columns of progenitors by 3 dpL. At 7 dpL, only a few remaining PCNA-positive progenitors remain in the outer nuclear layer (arrow; panel D). E) Graphic representation of changes in *shha*, *shhb*, *gli1*, and *ptch2* expression during the light treatment timecourse, with all time points performed in biological and technical triplicate and normalized to the expression of *gria*. Significantly different from 0 hr are noted with an asterisk ($p < 0.01$). Error bars represent standard error of the mean. ONL: outer nuclear layer, INL: inner nuclear layer, GCL: ganglion cell layer.



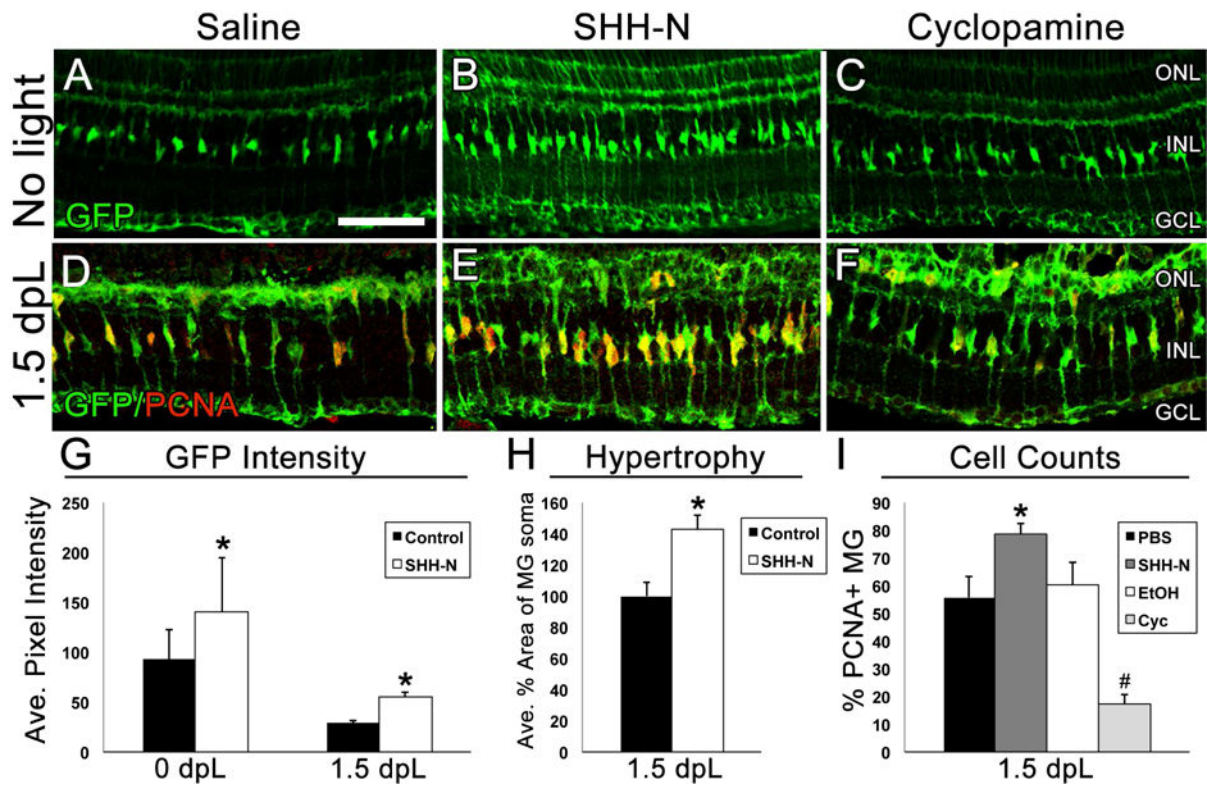


Figure 3. Müller glial cell reactivity in the retina following SHH-N treatment

A–C) Retinal sections showing GFP expression in Müller glial cells (green) in *Tg(gfap:egfp)* zebrafish in the absence of damage to represent changes in GFP intensity and changes in Müller glial cell morphology following treatment with saline, SHH-N or cyclophamide. D–F) Retinal sections from *Tg(gfap:egfp)* zebrafish immunolabeled with GFP to show Müller glial cells (green) and PCNA to show cell proliferation (red) at 1.5 dpL. G) Graphical representation of the average pixel intensity of GFP+ Müller glia as analyzed by Image J (N=5 per treatment group per timepoint). H) Graphical representation of average percent area of Müller glial soma as analyzed by ImageJ (N=5 per treatment group). I) Graphical representation of data showing that SHH-N significantly increased Müller glia proliferation (N=5 per treatment group; $p=0.028$), while cyclophamide significantly decreased Müller glia proliferation (N=5 per treatment group; $p=0.003$). ONL: outer nuclear layer, INL: inner nuclear layer, GCL: ganglion cell layer, ROS: rod outer segments.

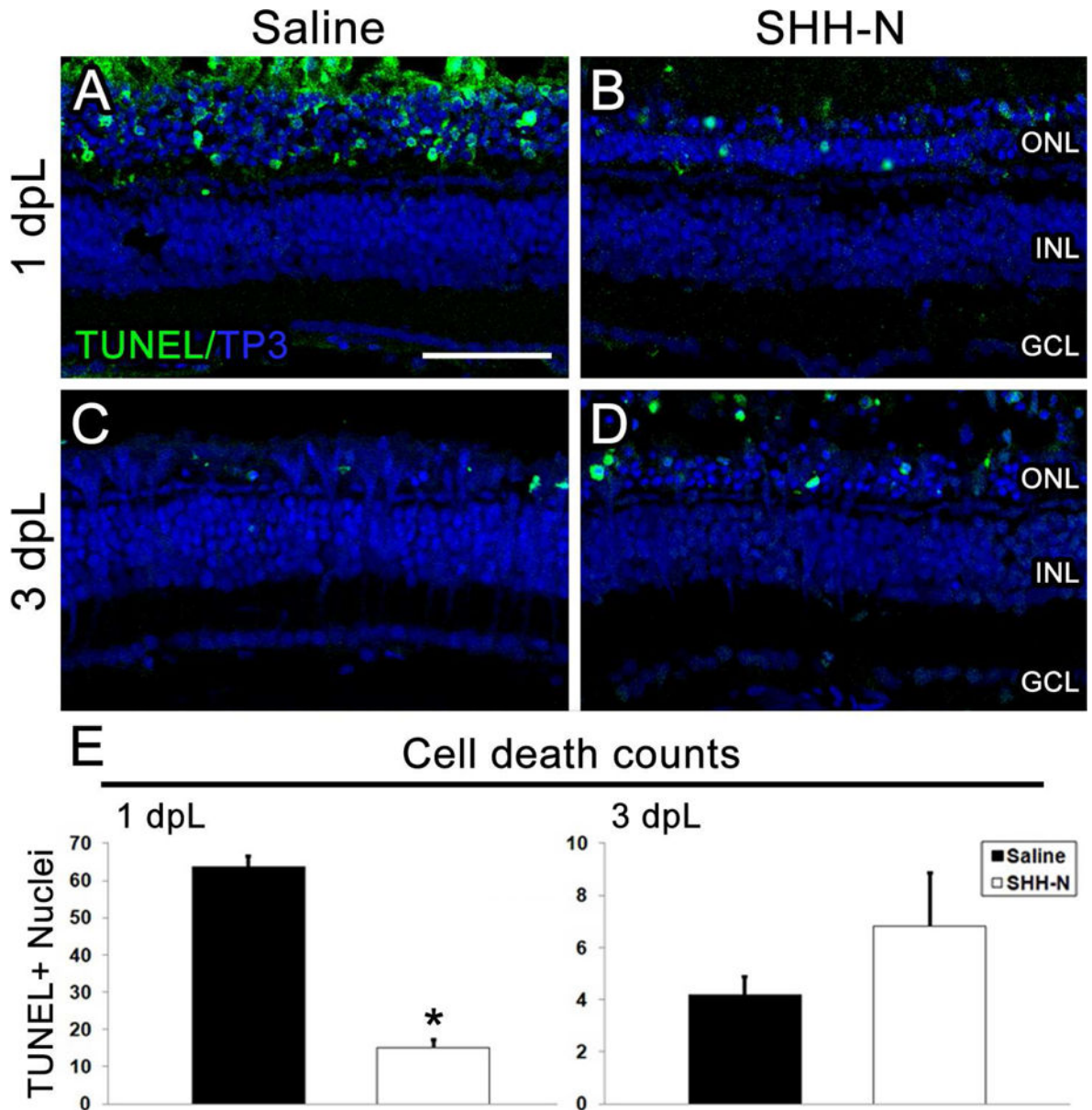


Figure 4. SHH-N treatment decreases cell death in the light damaged retina

A–D) TUNEL immunolocalization labels apoptotic cells (green). Nuclei are stained with TO-PRO-3 (blue). A–B) At 1 dpL, significantly fewer TUNEL-positive nuclei are observed in SHH-N treated retinas than saline injected. C–D) At 3 dpL, no significant changes are observed between treatment groups. E) Graph depicting the average number of TUNEL-positive cells in the ONL within a linear distance of 300 microns at 1 and 3 dpL. Significantly different from control is noted with an asterisk (N=5 per treatment group per time point; $p < 0.001$). Error bars represent standard error of the mean. ONL: outer nuclear layer. INL: inner nuclear layer. GCL: ganglion cell layer.

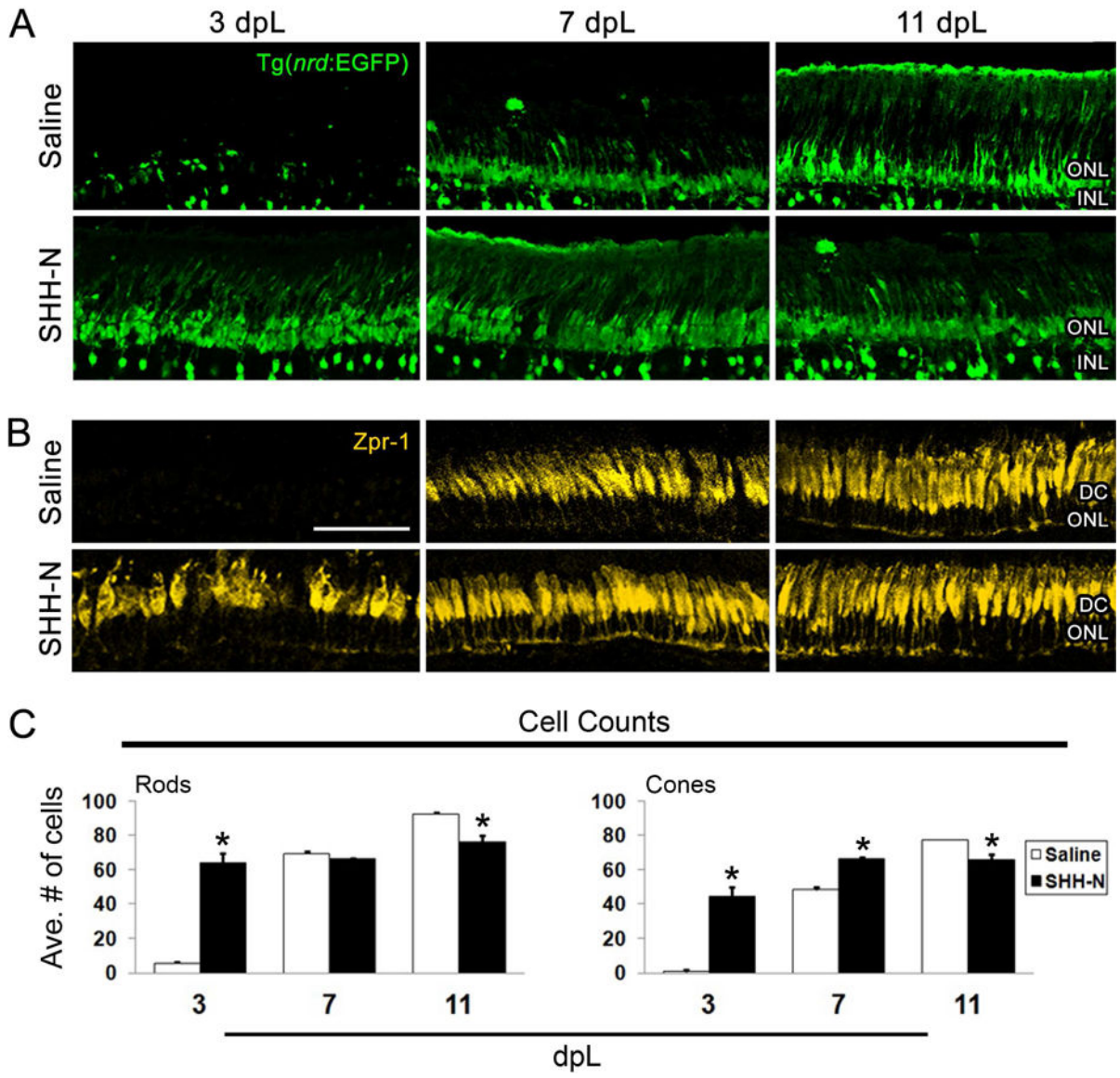


Figure 5. Photoreceptor regeneration in the light damaged retina following SHH-N treatment
 A–B) Retinal sections from *Tg(nrd:egfp)/alb* zebrafish immunolabeled with GFP to show rod photoreceptors and a subset of inner retinal neurons (green) or *Zpr-1* to show red/green double cones (yellow) at 3, 7 or 11 dpL following saline (top panels) or SHH-N treatment (bottom panels). SHH-N maintained photoreceptors at 3 dpL, but fewer remained at 11 dpL.
 C) Graph depicting the number of rod and cone photoreceptors at 3, 7 and 11 dpL in saline or SHH-N treated retinas. Significantly different from control is noted with an asterisk (N= 5 per treatment group per time point; $p < 0.01$). Error bars represent standard error of the mean. ONL: outer nuclear layer. INL: inner nuclear layer. DC: double cones.

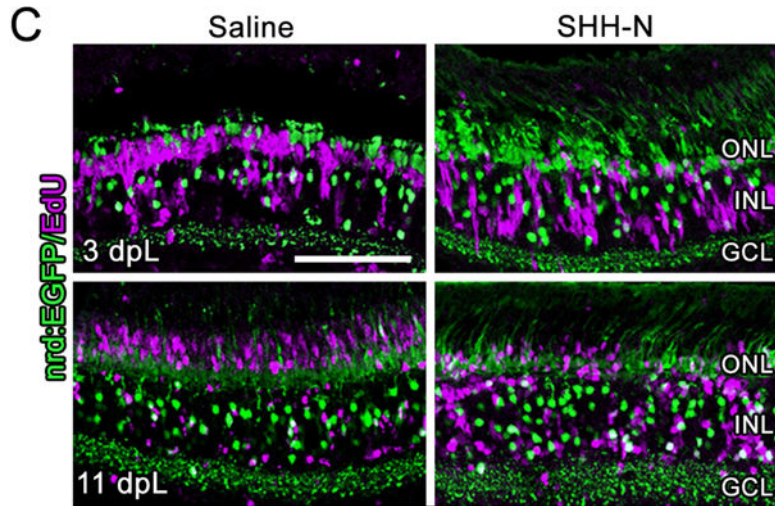


Figure 6. Increased inner retinal neuron regeneration following SHH-N treatment in the light damaged retina

A) Nuclei are stained with TO-PRO-3 (blue). Compared with control retinas (top panel), SHH-N-treated retinas have a thicker INL. B) Graph depicting the number of nuclei in the ONL, INL, and GCL at 11 dpL. C) GFP expression in the *Tg(nrd:egfp)/alb* zebrafish line to show rod photoreceptors and a subset of INL cells (green) co-localized with EdU to label cells that re-entered the cell cycle (purple). EdU-positive cells largely remained in the INL of SHH-N treated retinas. D) Graph depicting the number of EdU-positive cells at 11 dpL in the INL and ONL. E) EdU immunofluorescence (red) co-localized with HuC/D (blue) or PKC (teal) in SHH-N treated retinas shows EdU-positive cell largely co-labeled with amacrine cells (framed with bar), and only isolated bipolar cells (arrow). Significantly different from control is noted with an asterisk (N=5–6 per treatment group per time point; $p < 0.05$). Error bars represent standard error of the mean. ONL: outer nuclear layer. INL: inner nuclear layer. GCL: ganglion cell layer.

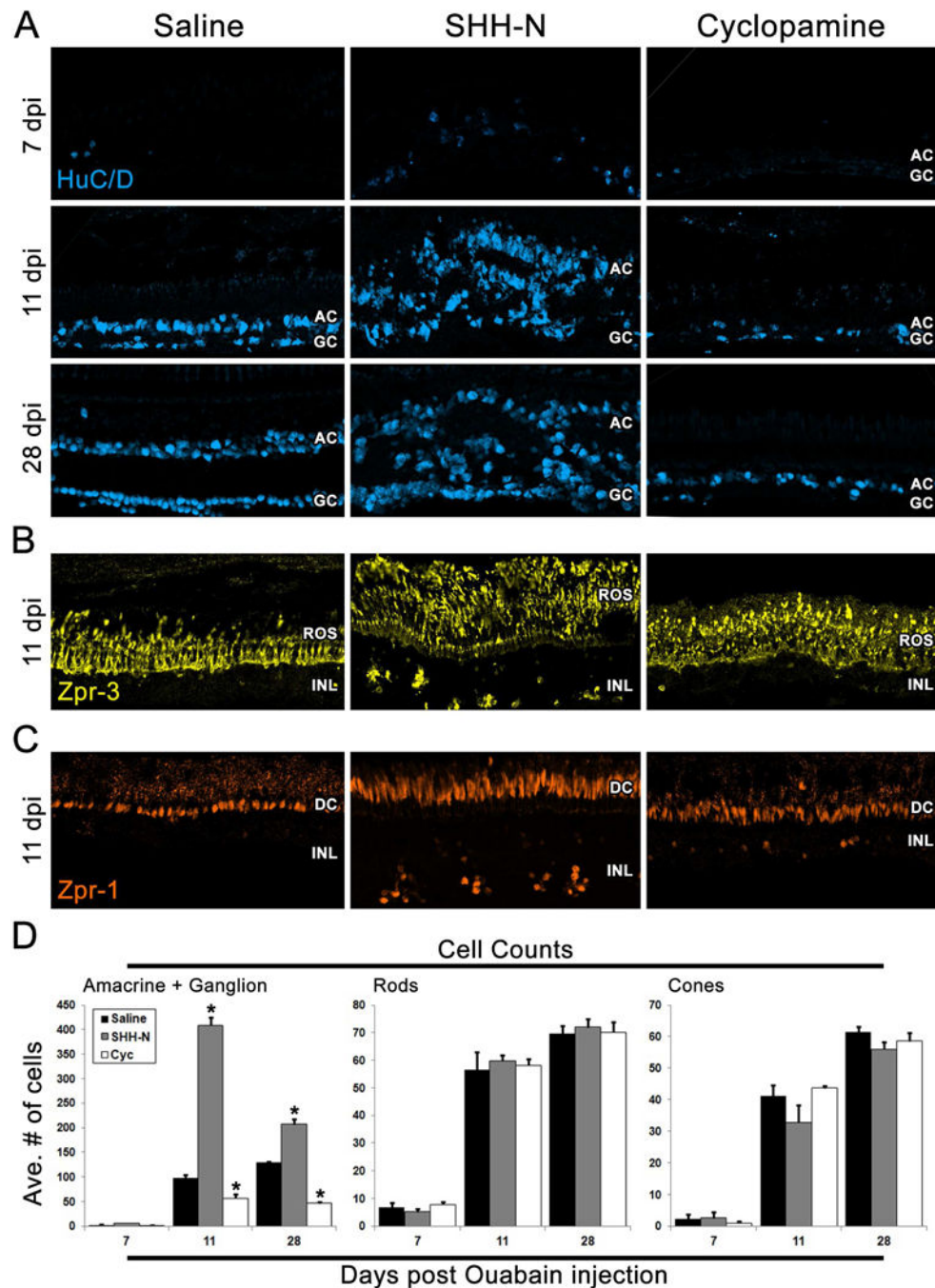


Figure 7. Retinal neuron regeneration in the Ouabain damaged retina following SHH-N or cyclopamine treatment

A–C) Retinal sections from saline, SHH-N or cyclopamine treated retinas immunolabeled with HuC/D to show amacrine and ganglion cells (A; blue), Zpr-3 to show rod photoreceptors (B, yellow) or Zpr-1 to show red/green double cones (C; orange). A) Changes in the number of differentiated amacrine and ganglion cells at 7, 11 and 28 dpi. B–C) No changes in the number of differentiated rod or cone photoreceptors in the ONL across treatment groups at 11 dpi. Note that SHH-N treated retinas exhibited “rosettes” of rod and cone photoreceptors in the INL, but these cells were not counted in our analysis, as they

were not located in the ONL. D) Graph depicting the number of regenerated amacrine and ganglion cells and rod and cone photoreceptors at 7, 11 and 28 dpi. Significantly different from control is noted with an asterisk(N=5 per treatment group per time point; $p < 0.05$). Error bars represent standard error of the mean. INL: inner nuclear layer. ROS: rod outer segments. DC: double cones. AC: amacrine cells. GC: ganglion cells.

Author Manuscript

Author Manuscript

Author Manuscript

Author Manuscript